SUPPLEMENTAL MATERIALS

ASCE *Journal of Geotechnical and Geoenvironmental Engineering*

Construction on Slow-Moving Landslides: Effects of Excavation on Neighboring Structures

Roman Hettelingh and Alexander M. Puzrin

DOI: 10.1061/JGGEFK.GTENG-11318

APPENDIX S1. INITIAL STRESS STATE

This section presents the derivations for the initial stress state of the modelled slopes and landslides.

Stable Slope Conditions

Consider an infinite half-space, representing a sloped ground inclined to the horizontal by an angle α. The assumed initial stress state of the slope will be discussed on both the soil element with vertical and horizontal sides (x-y-z coordinate system) and the soil element with slope parallel and slope perpendicular sides (t-y-n coordinate system), as shown in Figure S1.

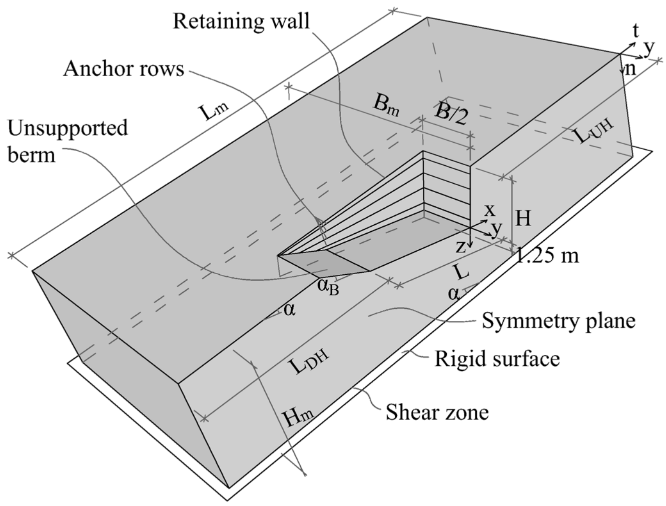

Figure S1. Geometry of the modelled landslide portion, the excavation pit, the retaining wall and the soil anchor rows.

The corresponding stress tensor is given by:

$$\boldsymbol{\sigma}^{\mathbf{0}}_{\boldsymbol{xyz}} = \begin{pmatrix} \sigma_x^0 & 0 & \tau_{xz}^0 \\ 0 & \sigma_y^0 & 0 \\ \tau_{xz}^0 & 0 & \sigma_z^0 \end{pmatrix} \qquad \boldsymbol{\sigma}^{\mathbf{0}}_{\boldsymbol{tyn}} = \begin{pmatrix} \sigma_t^0 & 0 & \tau_{tn} \\ 0 & \sigma_y^0 & 0 \\ \tau_{tn} & 0 & \sigma_n \end{pmatrix} \tag{S1}$$

The normal stress σ_n and the shear stress τ_{tn} are both given by equilibrium alone (Friedli, Hauswirth and Puzrin, 2017), while the normal stresses σ_t^0 and σ_y^0 result from the kinematic conditions $\varepsilon_t = 0$ and $\varepsilon_y = 0$ and the constitutive behaviour of the soil during the consolidation process. The stresses in the t-y-n coordinates are:

$$\begin{aligned} \sigma_n &= \gamma\, z \cos^2 \alpha \\ \tau_{tn} &= -\gamma\, z \sin\alpha \cos\alpha \\ \sigma_y^0 &= \sigma_t^0 = \overline{K}_0\, \sigma_n \\ n &= z \cos\alpha \end{aligned} \tag{S2}$$

where γ is the unit weight of the soil.

The factor $\overline{K}_0$ relates the slope-parallel and out of plane normal stresses σ_t^0 and σ_y^0 to the slope-perpendicular stress σ_n, and is assumed independent of the depth z. The idealized consolidation process of an infinite slope happens in a state of uniaxial normal strain ε_n (i.e. $\varepsilon_t = \varepsilon_y = 0$). Unlike on flat ground, the soil also exhibits the shear stress τ_{tn} and strain ε_{tn}, and it is unknown how this affects the evolution of σ_y^0. However, as will be shown below, σ_t^0 is larger in a slope than on flat ground, and due to the uniaxial strain condition it seems reasonable to assume that also σ_y^0 should be larger, with the simplest assumption being the equality of σ_y^0 and σ_t^0.

Tensor rotation yields the stresses in the x-y-z coordinates:

$$\sigma_x^0 = (\overline{K}_0 \ \cos^2\alpha - \sin^2\alpha)\cos^2\alpha\ \gamma\ z \tag{S3}$$

$$\sigma_z^0 = \big((2+\overline{K}_0)\sin^2\alpha + \cos^2\alpha\big)\cos^2\alpha\ \gamma\ z$$

$$\tau_{xz}^0 = -(\overline{K}_0\ \cos^2\alpha - \sin^2\alpha)\sin\alpha\cos\alpha\ \gamma\ z$$

$$\sigma_y^0 = \overline{K}_0\cos^2\alpha\ \gamma\ z$$

The earth pressure on a cut perpendicular to the x-direction, is commonly expressed with the earth pressure coefficient K_{0x}, defined as the earth pressure e_{0x} acting on that cut, normalized by $\gamma \cdot z$:

$$e_{0x} = \sqrt{(\sigma_x^0)^2 + (\tau_{xz}^0)^2} = K_{0x}\ \gamma\ z \tag{S4}$$

The definitions of σ_x^0 and τ_{xz}^0 from equations (S3) show that e_{0x} always acts in slope parallel direction:

$$\frac{\tau_{xz}^0}{\sigma_x^0} = -\tan\alpha \tag{S5}$$

Therefore, the horizontal (K_{ohx}) and vertical (K_{ovx}) components of K_{0x} are defined as:

$$K_{0hx} = K_{0x}\cos\alpha = \frac{\sigma_x^0}{\gamma\ z} \qquad K_{0vx} = K_{0x}\sin\alpha = \frac{-\tau_{xz}^0}{\gamma\ z} \tag{S6}$$

Concerning the earth pressure on a cut perpendicular to the y-direction, e_{0y}, K_{0y} and K_{0hy} are defined accordingly:

$$e_{0y} = \sigma_y^0 \tag{S7}$$

$$K_{0y} = K_{0hy} = \frac{\sigma_y^0}{\gamma\ z}$$

By comparing equations (S3) and (S6), $\overline{K}_0$ can be expressed through K_{0x} as follows:

$$\overline{K}_0 = \frac{K_{0x}}{\cos^3\alpha} + \tan^2\alpha \tag{S8}$$

Finally, using equations (S3), (S6), (S7) and (S8) the following expressions result for the stresses in the x-y-z coordinates:

$$\sigma_x^0 = K_{0hx}\,\gamma\, z = K_{0x}\cos\alpha\ \gamma\, z \tag{S9}$$

$$\sigma_z^0 = (1 + K_{0x}\sin\alpha\tan\alpha)\,\gamma\, z$$

$$\tau_{xz}^0 = -K_{0vx}\,\gamma\, z = -K_{0x}\sin\alpha\ \gamma\, z$$

$$\sigma_y^0 = K_{0y}\,\gamma\, z = \left(\frac{K_{0x}}{\cos\alpha} + \sin^2\alpha\right)\gamma\, z$$

K_{0x} can either be determined by modelling the consolidation process of the slope with an appropriate constitutive model, or a value can be taken from literature. Pursuing the latter approach, the K_{0x} for normally consolidated ground proposed by Franke (1974) is widely accepted in practice:

$$K_{0x} = \frac{(1 - \sin\varphi')\,(1 + \sin\alpha)}{\cos\alpha} \tag{S10}$$

For horizontal ground ($\alpha = 0$) it reduces to the abbreviated form of Jaky (1944):

$$K_{0x} = 1 - \sin\varphi' \tag{S11}$$

And for $\alpha = \varphi'$ it coincides with Rankine's solution (Rankine, 1857):

$$K_{0x} = \cos\varphi' \tag{S12}$$

For all other slope inclinations α it has been calibrated with experiments. Both the Swiss code SIA (Schweizerischer Ingenieur- und Architektenverein) (2020) and the European code CEN (European Committee for Standardization) (2004) have adopted the determination of K_{0x} according to equation (S10).

Landslide Conditions

Now, consider the same kind of slope, which has a slope parallel layer of thickness t_{sz} in a depth H_m, representing the shear zone with a strength of $\varphi'_{sz} = \alpha$. Assuming a material that fails according to the Mohr-Coulomb failure criterion, the stress state in the shear zone lies exactly on the failure surface, and can therefore undergo shear deformation ε_{tn} without changing the stress state of the whole slope, which is still the one according to equations (S2). The above considerations describe an idealization of an uncompressed, infinitely long and wide landslide. If the sliding mass is somehow constrained at the downslope end (e.g. by a rock outcrop, by decreasing slope inclination or by a retaining structure) and has parts which are unstable by themselves towards the uphill end (i.e. $\varphi'_{sz} < \alpha$), the sliding mass is in a compressed state in t-direction and the stress field is different from the one given in equations (S2). In the landslide part where $\varphi'_{sz} = \alpha$, both the slope parallel and the out-of-plane stresses σ_t and σ_y increase during compression, while σ_n and τ_{tn} remain the same as in equation (S2). A common assumption is that the slope compresses with roughly uniform ε_t over the landslide depth H_m, which is suggested by the affinity of several deformation profiles from inclinometer measurements along the slide (e.g. Cevasco *et al.*, 2018). Considering also the assumed linear stress dependency of stiffness, the compressed stress state is therefore:

$$\sigma_n = \gamma\, z \cos^2\alpha \tag{S13}$$

$$\tau_{tn} = -\gamma\, z \sin\alpha \cos\alpha$$

$$\sigma_t = \overline{K}_{tn}\, \sigma_n = \overline{K}_{tn}\, \gamma\, z \cos^2\alpha$$

$$\sigma_y = \overline{K}_{yn}\, \sigma_n = \overline{K}_{yn}\, \gamma\, z \cos^2\alpha$$

Here, $\overline{K}_{tn}$ and $\overline{K}_{yn}$ are the ratios between σ_t or σ_y and σ_n respectively, in the compressed slope. The stress σ_y is in general not assumed to stay the same as σ_t. Tensor rotation and the same deductions leading up to equations (S9) again yield the stresses in the x-y-z coordinates:

$$\sigma_x = K_{hx}\, \gamma\, z = K_x \cos\alpha\ \gamma\, z = (\overline{K}_{tn}\ \cos^2\alpha - \sin^2\alpha) \cos^2\alpha\ \gamma\, z \tag{S14}$$

$$\sigma_z = (1 + K_x \sin\alpha \tan\alpha)\, \gamma\, z = \left((2 + \overline{K}_{tn}) \sin^2\alpha + \cos^2\alpha\right) \cos^2\alpha\ \gamma\, z$$

$$\tau_{xz} = -K_{vx}\, \gamma\, z = -K_x \sin\alpha\ \gamma\, z = -(\overline{K}_{tn}\ \cos^2\alpha - \sin^2\alpha) \sin\alpha \cos\alpha\ \gamma\, z$$

$$\sigma_y = K_y\, \gamma\, z = \overline{K}_{yn} \cos^2\alpha\ \gamma\, z$$

According to Friedli, Hauswirth and Puzrin (2017) there is a maximum value which K_{hx} can reach, called *landslide pressure coefficient* K_{lhx}, which is defined by:

$$K_{lhx} = \frac{\sigma_x}{\gamma\, z} = \frac{\cos^4\alpha}{\cos^2\varphi'} \left[1 + \sqrt{1 - \cos^2\varphi'\ (1 + \tan^2\alpha)}\right]^2 \tag{S15}$$

$$K_{lx} = \frac{e_{lx}}{\gamma\, z} = \frac{K_{lhx}}{\cos\alpha}$$

$$\overline{K}_{ltn} = 2\ \frac{1 + \sqrt{1 - \cos^2\varphi'\ (1 + \tan^2\alpha)}}{\cos^2\varphi'} - 1$$

The earth pressure coefficient K_{hx} of a compressed landslide therefore lies somewhere in between K_{0hx} and K_{lhx}, which leads to the definition of the *landslide compression ratio* k_c:

$$k_c = \frac{K_{hx} - K_{0hx}}{K_{lhx} - K_{0hx}} = \frac{K_x - K_{0x}}{K_{lx} - K_{0x}} = \frac{\overline{K}_{tn} - \overline{K}_0}{\overline{K}_{ltn} - \overline{K}_0} \tag{S16}$$

Using K_{0x} according to equation (S10) and assuming a specific k_c is not enough to describe the whole stress state. While it is sufficient to calculate $\overline{K}_{tn}$ and therefore σ_t, the determination of σ_y requires knowledge about the constitutive behavior of the landslide mass during the compression process. The solution to this matter is presented in the main article.

APPENDIX S2. DAMAGE CATEGORIES AND LIMITING TENSILE STRAINS

The damage categories and the corresponding limiting tensile strains that were used in the main article are given in Table S1.

Table S1. Classification of visible damage to walls, using crack widths (after Burland, Broms and De Mello (1977)); limiting tensile strains leading to these cracks (Son and Cording, 2005).

Damage Category	Description of typical damage	Approximate individual crack width	Limiting tensile strain
Negligible (0)	-	$< 0.1\ mm$	$5.0 \cdot 10^{-4}$
Very slight (1)	Fine cracks which can easily be treated during normal decoration. Perhaps isolated slight fracture in building. Cracks in external brickwork visible on close inspection.	$0.1 \div 1\ mm$	$7.5 \cdot 10^{-4}$
Slight (2)	Cracks easily filled. Re-decoration probably required. Several slight fractures showing inside of building. Cracks are visible externally and some re-pointing may be required externally to ensure weather-tightness. Doors and windows may stick slightly.	$1 \div 5\ mm$	$1.67 \cdot 10^{-3}$
Moderate (3)	The cracks require some opening up and can be patched by a mason. Recurrent cracks can be masked by suitable linings. Repointing of external brickwork and possibly a small amount of brickwork to be replaced. Doors and windows sticking. Service pipes may fracture. Weathertight-ness often impaired.	$5 \div 15\ mm$ or a number of cracks $\geq 3\ mm$	$3.33 \cdot 10^{-3}$
Severe (4)	Extensive repair work involving breaking-out and replacing sections of walls, especially over doors and windows. Windows and door frames distorted, floor sloping noticeably. Walls leaning or bulging noticeably, some loss of bearing in beams. Service pipes disrupted.	$15 \div 25\ mm$, but also depends on number of cracks	$> 3.33 \cdot 10^{-3}$
Very severe (5)	This requires a major repair job involving partial or complete re-building. Beams lose bearing, walls lean badly and require shoring. Windows broken with distortion. Danger of instability.	usually $> 25\ mm$, but depends on number of cracks	$> 3.33 \cdot 10^{-3}$

APPENDIX S3. LAYOUT OF THE PARAMETRIC STUDY

Figure S2 shows all the calculated landslide model variations. For reference, a series of models with an excavation within a stable slope were also calculated (Figure S3). The models on stable flat ground were each run once with a berm on the downhill side, and once with a retaining wall on all four sides of the excavation (Figure S4). Another limited model series was run for reference, with stable slopes and anchor design for the full K_0 earth pressure, but with the anchor design done for a triangular earth pressure distribution (Figure S5).

Slope condition	Retaining structure	Earth pressure distribution for anchor design
Landslide	3 walls, 1 berm	Trapezoidal
Stable slope	4 walls	Triangular

Model dimensions	
$L_{UH} \approx 98 \div 120\ m$	$B_m = 150\ m$
$L_{DH} \approx 98 \div 120\ m$	$H_m = 20\ m$

α	φ'		
	25°	30°	35°
10°	x	x	
15°	x	x	x
20°		x	x

k_c	f_{a-0}^{anch}		f_{0-l}^{anch}					
	0.0	0.25	0.0	0.2	0.4	0.6	0.8	1.0
0.0		x	x					
0.2		x	x	x				
0.4		x	x	x	x			
0.6		x	x	x	x	x		
0.8		x	x	x	x	x	x	
1.0					x	x	x	x

Figure S2. Landslide models → $7 \times 24 = 168$ models

Slope condition	Retaining structure	Earth pressure distribution for anchor design	Model dimensions	
Landslide	3 walls, 1 berm	Trapezoidal	$L_{UH} \approx 160 \div 170\ m$	$B_m = 100\ m$
Stable slope	4 walls	Triangular	$L_{DH} \approx 100 \div 115\ m$	$H_m = 60\ m$

α	φ'		
	25°	30°	35°
0°	x	x	x
10°	x	x	
15°	x	x	x
20°		x	x

k_c	f_{a-0}^{anch}		f_{0-l}^{anch}
	0.0	0.25	0.0
0.0		x	x

Figure S3. Stable slope models → $10 \times 2 = 20$ models

Slope condition	Retaining structure	Earth pressure distribution for anchor design	Model dimensions	
Landslide	3 walls, 1 berm	Trapezoidal	$L_{UH} = 90\ m$	$B_m = 100\ m$
Stable slope	4 walls	Triangular	$L_{DH} = 90\ m$	$H_m = 60\ m$

α	φ'		
	25°	30°	35°
0°	x	x	x

k_c	f_{a-0}^{anch}		f_{0-l}^{anch}
	0.0	0.25	0.0
0.0		x	x

Figure S4. Flat stable ground models with a retaining wall on all four sides → $4 \times 2 = 8$ models

Slope condition	Retaining structure	Earth pressure distribution for anchor design
Landslide	3 walls, 1 berm	Trapezoidal
Stable slope	4 walls	Triangular

Model dimensions	
$L_{UH} \approx 160 \div 170\ m$	$B_m = 100\ m$
$L_{DH} \approx 100 \div 107\ m$	$H_m = 60\ m$

α	φ'
	30°
0°	x
10°	x
15°	x
20°	x

k_c	f_{0-l}^{anch}
	0.0
0.0	x

Figure S5. Stable slope models with triangular earth pressure distribution → 4 × 1 = 4 models

APPENDIX S4. DISPLACEMENT FIELD AROUND EXCAVATION

This section aims to help understand the maximum tensile strains $\varepsilon^{t}{}_{m}{}^{ot}{}_{ax}$ generated in the building walls, from a depiction of the displacement field in the uphill sector of the excavation. Figure S6 shows the displacement magnitude field on central cuts through the excavation pit at the end of the excavation for differently inclined slopes, each with $\varphi' = 30^{\circ}$. The larger the slope inclination α, the larger the moving wedge in the uphill sector, and thus the further the reach of displacements in uphill direction. What plays a further big role is the way $\varepsilon^{t}{}_{m}{}^{ot}{}_{ax}$ is evaluated in this study, i.e. on the neighbouring building base. The positioning of neighboring buildings, indicated in Figure S6, explains the negligible damage for $\alpha = 0$ and the growing reach with increasing α, as well as the high magnitudes for close distances d for moderate α.

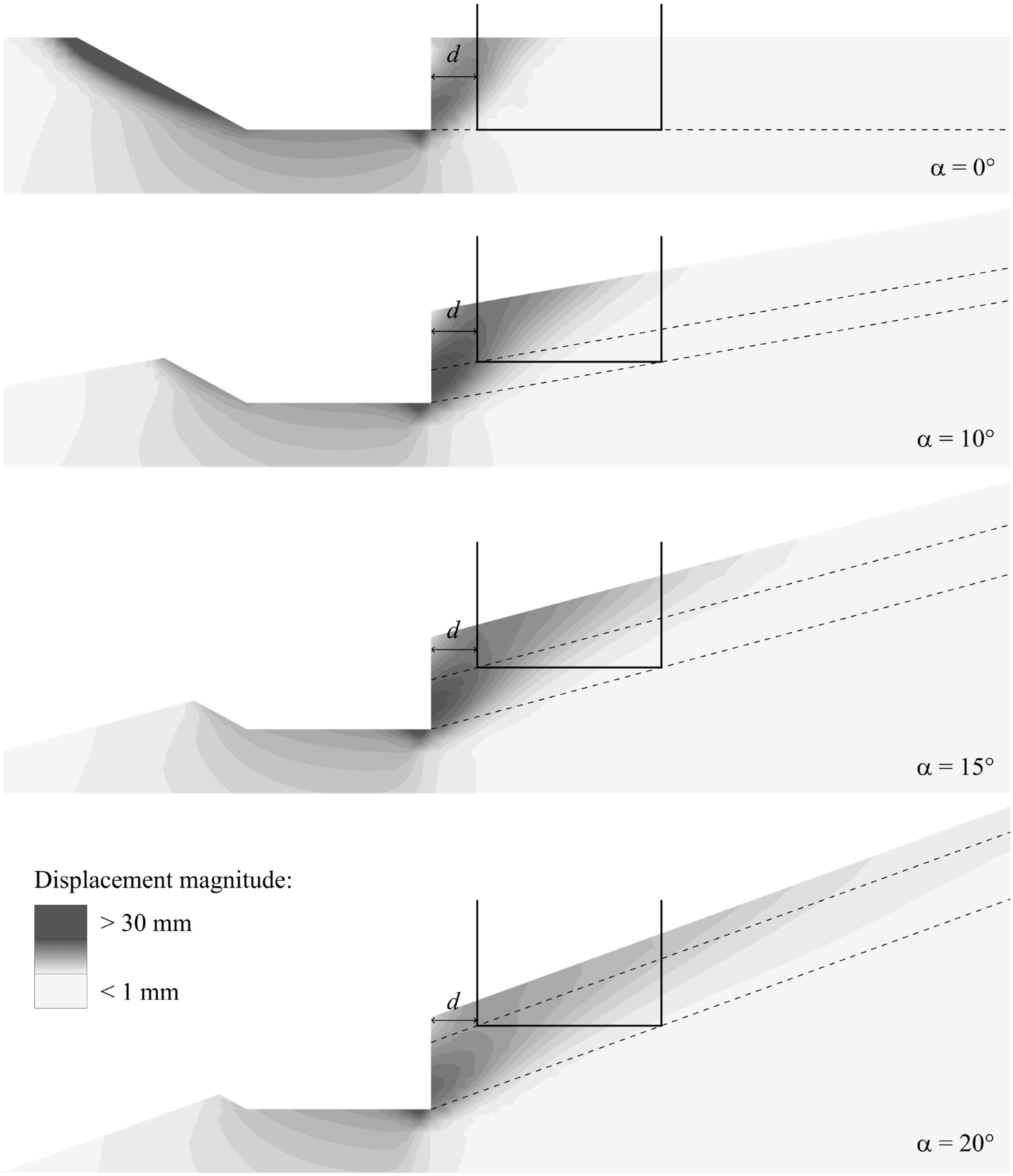

Figure S6. Displacement magnitude field around excavations in stable slopes with various slope inclinations α, each with $\varphi' = 30^{\circ}$.

REFERENCES

Burland, J.B., Broms, B.B. and De Mello, V.F.B. (1977) 'Behaviour of foundations and structures', in *Proc. 9th International Conference on Soil Mechanics and Foundation Engineering, Tokyo, Japan, 1977*. Tokyo: Japanese Society of Soil Mechanics and Foundation Engineering, pp. 495–546.

CEN (European Committee for Standardization) (2004) *Eurocode 7: Geotechnical design - Part 1: General rules. (EN 1997-1)*. Brussels: CEN.

Cevasco, A., Termini, F., Valentino, R., Meisina, C., Bonì, R., Bordoni, M., Chella, G.P. and De Vita, P. (2018) ‘Residual mechanisms and kinematics of the relict Lemeglio coastal landslide (Liguria, northwestern Italy)’, *Geomorphology*, 320, pp. 64–81. Available at: https://doi.org/10.1016/j.geomorph.2018.08.010.

Franke, E. (1974) ‘Ruhedruck in kohäsionslosen Böden’, *Bautechnik*, 51(1), pp. 18–24. Available at: https://structurae.net/en/literature/journal-article/ruhedruck-in-kohasionslosen-boden (Accessed: 1 April 2021).

Friedli, B., Hauswirth, D. and Puzrin, A.M. (2017) ‘Lateral earth pressures in constrained landslides’, *Géotechnique*, 67(10), pp. 1–16. Available at: https://doi.org/10.1680/jgeot.16.P.158.

Jaky, J. (1944) ‘The coefficient of earth pressure at rest. In Hungarian (A nyugalmi nyomas tenyezoje).’, *Journal of Society of Hungarian Architects and Engineers (Magyar Mernok es Epitesz-Egylet Kozlonye)*, 78(22), pp. 355–358.

Rankine, W.J.M. (1857) ‘On the Stability of Loose Earth’, *Philosophical Transactions of the Royal Society of London*, 147(0), pp. 9–27. Available at: https://doi.org/10.1098/rstl.1857.0003.

SIA (Schweizerischer Ingenieur- und Architektenverein) (2020) *Einwirkungen auf Tragwerke. (SIA 261. SN 505 261)*. Zurich: SIA.

Son, M. and Cording, E.J. (2005) ‘Estimation of Building Damage Due to Excavation-Induced Ground Movements’, *Journal of Geotechnical and Geoenvironmental Engineering*, 131(2), pp. 162–177. Available at: https://doi.org/10.1061/(ASCE)1090-0241(2005)131:2(162).